Deep Learning Based Robust Precoding for Massive MIMO

Junchao Shi, *Student Member, IEEE*, Wenjin Wang, *Member, IEEE*, Xinping Yi, *Member, IEEE*, Xiqi Gao, *Fellow, IEEE*, and Geoffrey Ye Li, *Fellow, IEEE*

***Abstract*—In this paper, we consider massive multiple-input-multiple-output (MIMO) communication systems with a uniform planar array (UPA) at the base station (BS) and investigate the downlink precoder design with imperfect channel state information (CSI). By exploiting channel estimates and statistical parameters of channel estimation error, we aim to design precoding vectors to maximize the utility function on the ergodic rates of users subject to a total transmit power constraint. By employing an upper bound of the ergodic rate, we leverage the corresponding Lagrangian formulation and identify the structural characteristics of the optimal precoder as the solution to a generalized eigenvalue problem. The Lagrange multipliers play a crucial role in determining both precoding directions and power parameters, yet are challenging to be solved directly. To figure out the Lagrange multipliers, we develop a general framework underpinned by a properly designed neural network that learns directly from CSI. To further relieve the computational burden, we obtain a low-complexity framework by decomposing the original problem into computationally efficient subproblems with instantaneous and statistical CSI handled separately. With the offline pre-trained neural network, the online computational complexity of precoder is substantially reduced compared with the existing iterative algorithm while maintaining nearly the same performance.**

***Index Terms*—Robust precoding, precoding structure, deep learning, massive MIMO**

I. Introduction

By deploying a large number of antennas at the base station (BS), massive multiple-input-multiple-output (MIMO) technique improves spectrum efficiency while serving multiple users at the same time [2]. With a vast number of antennas, either in a linear or planar array, the BS can steer the precoding directions accurately to alleviate the interference among users.

Over the past several years, downlink precoder design for massive MIMO has attracted extensive interest [3]. In quasi-static and low-mobility scenarios, the available instantaneous channel state information (CSI) at the BS is relatively accurate. In this situation, linear precoding methods, e.g., regularized zero-forcing (RZF), signal-to-leakage-and-noise ratio (SLNR), and weighted minimum mean-squared error (WMMSE) [4]–[6], can easily achieve multiplexing gain [7]. The maximum sum rate can also be achieved by using MAC-BC duality iterative water filling [8]–[10]. The monotonic optimization (MO) algorithms can obtain the global optimal solution to the secrecy sum rate maximization problem while the sequential parametric convex approximation (SPCA) algorithm balances the complexity and the performance [11].

The performance of precoders depends on the accuracy of available instantaneous CSI at the transmitter (CSIT) [12]. Its availability relies on downlink estimation and uplink feedback in a frequency division duplexing system. Nevertheless, it is challenging to obtain the perfect CSIT in practical systems due to heavy pilot overhead [13] and channel estimation errors [14], etc. Furthermore, for high-mobility scenarios, relatively short channel coherence time also results in more challenges on CSI acquisition. In brief, CSIT obsolescence and error often incur severe performance degradation for the precoders relying highly on instantaneous CSI (ICSI).

The recent work in [15] has designed a robust precoder that combines the channel estimates and statistical parameters of channel estimation error into a posteriori channel model. The statistical parameters of channel estimation error are modeled as the scaled statistical CSI. Instantaneous CSI varies with time while statistical CSI (SCSI) usually changes slowly. The posteriori channel model can adapt to the change of the varying communication environment. The spatial domain correlation characteristics [16] can be further used to address the effects of channel estimation error and channel ageing.

While the use of statistical CSI lends itself to robustness in precoder design, it requires to average the computation over a large number of channel samples to reach the corresponding ergodic rate, which is challenging. The iterative algorithm in [17] can achieve near-optimal performance at the expense of high computational complexity and processing delay.

The recent success of deep learning in many related areas has motivated its exploration in wireless communications [18], including channel estimation [19], signal detection [20], [21],

This work was supported in part by the National Key R&D Program of China under Grant 2018YFB1801103, the Jiangsu Province Basic Research Project under Grant BK20192002, the National Natural Science Foundation of China under Grants 61631018 and 61761136016, and the Huawei Cooperation Project. The work of X. Yi was supported in part by the Royal Society International Exchanges Scheme under award IEC\NSFC\201080. This article was presented in part at the IEEE International Conference on Communications (ICC), Montreal, QC, Canada, 2021 [1]. The associate editor coordinating the review of this article and approving it for publication was Prof. Rafael Schaefer. (Corresponding author: Xiqi Gao.)

J. Shi, W. Wang, and X. Q. Gao are with the National Mobile Communications Research Laboratory, Southeast University, Nanjing 210096, China, and also with the Purple Mountain Laboratories, Nanjing 211100, China (e-mail: jcshi@seu.edu.cn; wangwj@seu.edu.cn; xqgao@seu.edu.cn).

X. Yi is with the Department of Electrical Engineering and Electronics, University of Liverpool, Liverpool L69 3BX, United Kingdom (e-mail: xinping.yi@liverpool.ac.uk).

G. Y. Li is with the Department of Electrical and Electronic Engineering, Imperial College London, London SW7 2AZ, United Kingdom (e-mail: Geoffrey.Li@imperial.ac.uk).

Color versions of one or more of the figures in this paper are available online at http://ieeexplore.ieee.org.

precoding [22], end-to-end systems [23], [24], resource allocation [25], [26], etc. Specially for precoding, a multi-target precoder based on a unified deep neural network is designed in [27], [28], which reduces the computational complexity by more than one order of magnitude. A neural network structure, called auto-precoder, is proposed in [29], which can jointly sense millimeter-wave channels and design a hybrid precoding matrix with only a few training pilots. In [30], DNN based training is used to select the hybrid precoder to optimize the precoding process of mm-wave massive MIMO. The recent work in [31] has used deep learning for downlink beamforming with instantaneous CSI. The end-to-end learning model in [32] jointly optimizes the weights of transmitter and receiver networks in wireless channels. However, perfect CSI is required in these methods.

We aim to investigate deep learning for low-complexity robust precoder design. Despite many successful cases in deep learning for wireless communications [33], if not infeasible, it is challenging, to use deep learning for precoder design for the high dimensional precoding vectors as the output makes neural networks difficult to be trained. The numerical algorithm proposed in [34] uses a modified iterative water-filling approach based on a Lagrangian dual decomposition technique for the Gaussian multiple-access channel. To minimize the transmission powers while ensuring the SINR of each user, efficient algorithms have been proposed in [35] for the optimal beamforming problem. Based on an equivalent QoS problem of sum rate maximization problem, a simple structure of precoding vectors is provided in [36]. Note that the perfect CSI is assumed in [34]–[36] while we aim to investigate the precoding structure with imperfect CSI and find a way to convert the high-dimensional precoding problem into a low-dimensional parameter-learning one.

In this paper, we consider the posteriori channel model and formulate robust precoder design as the problem of maximizing the utility function on ergodic rates of users subject to a power constraint. To make this problem tractable, we employed an upper bound of the ergodic rate instead and transform it into an improved Quality-of-Service (QoS) problem, by which the structure of optimal precoding vectors is characterized. The proposed structure can successfully reduce the dimension of the problem and achieve outstanding performance. In summary, our contributions in this work are three-fold.

- By a Lagrangian formulation, we characterize the structure of optimal precoding vectors, whose direction and power can be associated with the solution to a generalized eigenvalue problem. Once the Lagrange multipliers are determined, the precoding vectors can be immediately computed, which transforms the high-dimensional precoder design problem into the low-dimensional Lagrange multipliers design problem.
- To determine the Lagrange multipliers, we use neural networks to learn the mapping from CSI to Lagrange multipliers, and therefore can immediately obtain the precoding vectors.
- We develop a low-complexity framework and decompose the original problem into two parts with instantaneous and statistical CSI-based precoders designed separately. Thus, two Lagrange set of multipliers are computed respectively, followed by a weighted combination.

Compared with the existing methods, the proposed framework significantly reduces the computational complexity while maintaining near-optimal performance.

The rest of this paper is organized as follows. In Section II, we present the posteriori channel and signal model. In Section III, we formulate the problem and further investigate the optimal solution structure. In Section IV, we develop a general framework for robust precoder design based on neural networks. In Section V, we develop a low-complexity framework to further reduce the computational complexity. Simulation results are presented in Section VI and the paper is concluded in Section VII.

Some of the notations used in this paper are listed as follows:

- Upper and lower case boldface letters denote matrices and column vectors, respectively.
- $\mathbb{C}^{M\times N}$ ($\mathbb{R}^{M\times N}$) denotes the $M\times N$ dimensional complex (real) matrix space, $(\cdot)^H$, $(\cdot)^T$, and $(\cdot)^*$ denote conjugate transpose, transpose, and complex conjugate operations, respectively.
- $\mathbb{E}\{\cdot\}$ denotes the expectation operation, $\mathbf{I}_N$ denotes the $N\times N$ identity matrix and the subscript for dimension is sometimes omitted for brevity.
- $\odot$ and $\otimes$ denote the Hadamard and Kronecker product of two matrices, respectively.
- $[\cdot]_i$ and $[\cdot]_{ij}$ denote the i-th element of a vector and the (i,j)-th element of a matrix, respectively, $\mathrm{tr}(\cdot)$ and $\det(\cdot)$ represent matrix trace and determinant operations, respectively.
- $\sim$ denotes 'be distributed as', $\triangleq$ denotes the definition, $\mathcal{CN}(\boldsymbol{\alpha},\mathbf{B})$ denotes the circular symmetric complex Gaussian distribution with mean $\boldsymbol{\alpha}$ and covariance $\mathbf{B}$.
- The inequality $\mathbf{A}\succeq\mathbf{0}$ means that $\mathbf{A}$ is Hermitian positive semi-definite.

II. System and Channel Models

The uniform planar array (UPA) is a typical array for massive MIMO systems due to its advantages such as high directivity [37], [38]. Thus, in this paper, we assume a uniform planar array at the base station. Consider downlink transmission of massive MIMO consisting of one BS and K users. The BS is equipped with an $M_v\times M_h$ uniform planar array, where M_v and M_h denote the numbers of vertical column and horizontal row, respectively. Thus, the number of antennas at the BS is $M_t=M_vM_h$. Each UE is equipped with a single antenna. For a time division duplexing (TDD) system, downlink and uplink transmissions are organized into slots, each consisting of N_b blocks. As can be illustrated in Fig. 1, in each slot, the blocks can be classified as 'uplink', or 'downlink' [39] for uplink sounding and downlink transmission, respectively. The first block of each slot contains the uplink sounding signal.

This article has been accepted for publication in a future issue of this journal, but has not been fully edited. Content may change prior to final publication. Citation information: DOI 10.1109/TCOMM.2021.3105569, IEEE Transactions on Communications

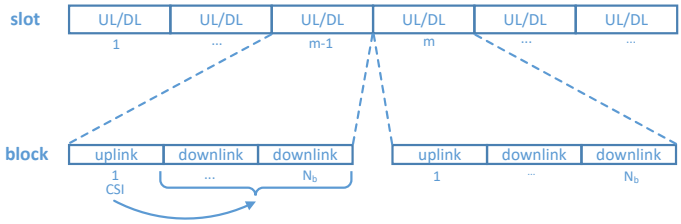

Fig. 1. Time frame structure of TDD systems.

A. Channel Model

The widely-adopted jointly correlated channel model in [16] uses the discrete Fourier transform (DFT) matrix to represent the spatial sampling matrix, which can model the physical channel accurately for uniform linear arrays with massive antennas. However, due to the limited antennas at each column or each row for uniform planar arrays, the simple solution of the Kronecker product extension of the DFT matrices may deviate from the physical model. Thus, we replace the DFT matrix with the oversampling one to capture the spatial correlation more precisely. Denote $N = N_h N_v$, where N_h and N_v are the vertical and horizontal oversampling factors, respectively. The spatial sampling matrix can therefore be represented by [17], [40]

$$\mathbf{V}_{M_t} = \mathbf{V}_{M_h} \otimes \mathbf{V}_{M_v} \in \mathbb{C}^{M_t \times N M_t}, \tag{1}$$

where the oversampling DFT matrices for the horizontal and vertical directions are respectively given by

$$\mathbf{V}_{M_h} = \frac{1}{\sqrt{M_h}} \left(e^{\frac{-j2\pi mn}{N_h M_h}} \right)_{m=0,\ldots,M_h-1, n=0,\ldots,N_h M_h-1}, \tag{2}$$

and

$$\mathbf{V}_{M_v} = \frac{1}{\sqrt{M_v}} \left(e^{\frac{-j2\pi mn}{N_v M_v}} \right)_{m=0,\ldots,M_v-1, n=0,\ldots,N_v M_v-1}. \tag{3}$$

It is assumed that the channel keeps unchanged at each block and varies across blocks, so that the precoder is carried once at each block. The obtained channel estimation at the first block will be used for the current slot. Thus, to capture the correlation across different blocks, the channel of the k-th user at the n-th block of the m-th slot can be represented by the posteriori model [17]

$$\mathbf{h}_{k,m,n} = \beta_{k,m,n} \bar{\mathbf{h}}_{k,m} + \sqrt{1-\beta_{k,m,n}^2} \mathbf{V}_{M_t} (\mathbf{m}_k \odot \mathbf{w}_{k,m,n}) \in \mathbb{C}^{M_t \times 1}, \tag{4}$$

where $\bar{\mathbf{h}}_{k,m}$ denotes the channel estimate, $\mathbf{m}_k \in \mathbb{C}^{NM_t \times 1}$ is a deterministic vector with nonnegative elements, $\mathbf{w}_{k,m,n} \in \mathbb{C}^{NM_t \times 1}$ is a complex Gaussian random vector of independent and identically distributed (i.i.d.) entries with zero mean and unit variance. The time correlation coefficient, $\beta_{k,m,n} \in [0,1]$, describes the uncertainty of the channel. The more severe the channel aging is, the more inaccurate the channel could be, i.e. the smaller the $\beta_{k,m,n}$ value. By adjusting $\beta_{k,m,n}$, the posteriori model can leverage channel uncertainties in various mobile scenarios, e.g., $\beta_{k,m,n} = 1$ corresponds to a quasi-static scenario where the channel is precisely known, and $\beta_{k,m,n} = 0$ corresponds to a high-mobility scenario where the channel is obsolete and only the statistical CSI is known. In this paper, we use the correlation coefficient between channels to characterize the channel uncertainty. Since only the estimated channel at the first block of each slot is available at the base station, we compute the correlation coefficients of the estimated channel between the current slot and the previous slot and then the correlation coefficients between the blocks are obtained by uniform interpolation, i.e., $\beta_{k,m,n} = 1 - \frac{n-1}{N_b}\left(1 - \frac{|\bar{\mathbf{h}}_{k,m-1}^H \bar{\mathbf{h}}_{k,m}|}{\|\bar{\mathbf{h}}_{k,m-1}\| \|\bar{\mathbf{h}}_{k,m}\|}\right)$.

Define the channel coupling vectors [41] as $\boldsymbol{\omega}_k = \mathbf{m}_k \odot \mathbf{m}_k$, where $[\boldsymbol{\omega}_k]_n$ indicates the average amount of energy that is coupled from the n-th spatial beam of the base station to the k-th user. Assume that $\bar{\mathbf{h}}_{k,m}$ and $\boldsymbol{\omega}_k$ are known at the base station through the channel sounding process. The posteriori model covers both the large-scale and small-scale fading [42], where the large-scale fading coefficient is embedded in $\boldsymbol{\omega}_k$. As the large-scale fading factor varies slow, we assume that $\boldsymbol{\omega}_k$ is constant within a relatively long period.

B. Downlink Transmission

We now consider the downlink transmission in one block of one slot. As the precoding method is uniform for arbitrary block, we omit m and n in the subscript hereafter. Denote x_k the transmitted signal to the k-th user, satisfying $\mathbb{E}\{|x_k|^2\} = 1$. The received signal of the k-th user is given by

$$y_k = \mathbf{h}_k^H \mathbf{p}_k x_k + \sum_{j \neq k}^{K} \mathbf{h}_k^H \mathbf{p}_j x_j + n_k, \tag{5}$$

where $\mathbf{p}_k \in \mathbb{C}^{M_t \times 1}$ is the precoding vector of the k-th user, and $n_k \sim \mathcal{CN}(0, \sigma_n^2)$ is a complex Gaussian noise. As the noise variances can be absorbed by the channel vectors, we here assume the noise variances of different users are the same without loss of generality [43]. In addition, we treat the aggregate interference-plus-noise $\sum_{j \neq k}^{K} \mathbf{h}_k^H \mathbf{p}_j x_j + n_k$ as Gaussian noise, and its covariance can be expressed as

$$r_k = \sigma_n^2 + \sum_{i \neq k}^{K} \mathbb{E}\{\mathbf{h}_k^H \mathbf{p}_i \mathbf{p}_i^H \mathbf{h}_k\}. \tag{6}$$

By assume that the covariance r_k is known at the k-th user, the ergodic achievable rate of the k-th user is given by [8], [17], [44]

$$\mathcal{R}_k = \mathbb{E}\Big\{ \log\left(1 + r_k^{-1} \mathbf{h}_k^H \mathbf{p}_k \mathbf{p}_k^H \mathbf{h}_k\right) \Big\}. \tag{7}$$

III. Optimal Precoding Structure Analysis

In this section, we formulate the robust precoding problem and characterize the structure of optimal precoding vectors by employing an upper bound of the ergodic rate.

A. Problem Formulation

The objective is to design precoding vectors $\mathbf{p}_1, \ldots, \mathbf{p}_K$ that maximize an utility function on ergodic rates of users as follows

$$\max_{\mathbf{p}_1,\ldots,\mathbf{p}_K} f(\mathcal{R}_1, \ldots, \mathcal{R}_K),$$

$$\text{s.t.} \quad \sum_{k=1}^{K} \mathbf{p}_k^H \mathbf{p}_k \leq P, \quad k = 1, \ldots, K, \tag{8}$$

where $f(\mathcal{R}_1, \ldots, \mathcal{R}_K)$ can be any function, e.g, sum rate, $\sum_{k=1}^{K} \mathcal{R}_k$, for overall data rate, and minimum rate, $\min_k \mathcal{R}_k$, for fairness among users, and P denotes the total power budget. Focusing on the ergodic rate efficiency, the precoding vectors satisfy widely-adopted total power constraint.

This optimization problem involves high-dimensional variables, and the objective function is non-convex in general. As a result, the exact solution is intractable. Although there exist various approximation methods, the high dimensionality of the optimization variables usually demands high computation to achieve optimal performance. For example, the iterative approach in [17] can nearly achieve the maximum sum rate. To reduce computational complexity, we aim to explore a solution structure of the precoding vectors to transform the high-dimensional optimization problem to a low-dimensional one.

B. Problem Transformation

As there exists no closed-form of the ergodic rate, direct optimization is intractable. Thus, we employ the following upper bound

$$\mathcal{R}_k \leq \mathcal{R}_k^{ub} \triangleq \log\left(1 + r_k^{-1} \mathbb{E}\{\mathbf{h}_k^H \mathbf{p}_k \mathbf{p}_k^H \mathbf{h}_k\}\right), \tag{9}$$

which is due to Jensen's inequality, making the problem more tractable. The optimization problem can be reformulated as

$$\mathbf{P1}: \quad \max_{\mathbf{p}_1, \ldots, \mathbf{p}_K} f(\mathcal{R}_1^{ub}, \ldots, \mathcal{R}_K^{ub}), \quad \text{s.t.} \quad \sum_{k=1}^{K} \mathbf{p}_k^H \mathbf{p}_k \leq P, \quad k = 1, \ldots, K. \tag{10}$$

Define the signal-to-interference-plus-noise-ratio (SINR) of the k-th user by

$$\text{SINR}_k = \frac{\mathbf{p}_k^H \mathbf{R}_k \mathbf{p}_k}{\sigma_n^2 + \sum_{i \neq k}^{K} \mathbf{p}_i^H \mathbf{R}_k \mathbf{p}_i}, \tag{11}$$

where $\mathbf{R}_k = \mathbb{E}\{\mathbf{h}_k \mathbf{h}_k^H\} \in \mathbb{C}^{M_t \times M_t}$. We have $\mathcal{R}_k^{ub} = \log(1 + \text{SINR}_k)$. Next, we introduce the following lemma to bridge our formulation to a QoS problem, proved in Appendix A.

Lemma 1: Denote $\gamma_1, \ldots, \gamma_K$ the SINR achieved by a solution (referred to as $\mathbf{S1}$) of $\mathbf{P1}$. The optimal solution (referred to as $\mathbf{S2}$) of the following QoS problem achieves the same ergodic rate upper bounds as $\mathbf{S1}$ but with lower or equal total power.

$$\mathbf{P2}: \quad \min_{\mathbf{p}_1, \ldots, \mathbf{p}_K} \sum_{k=1}^{K} \mathbf{p}_k^H \mathbf{p}_k, \quad \text{s.t.} \quad \text{SINR}_k \geq \gamma_k, \quad k = 1, \ldots, K. \tag{12}$$

When $\mathbf{S1}$ is the global optimal, $\mathbf{S2}$ is equivalent to $\mathbf{S1}$, i.e., achieves the same ergodic rate upper bounds and total power.

Lemma 1 indicates $\mathbf{P2}$ can improve or maintain any solution of $\mathbf{P1}$. In the original problem, the ergodic rates (upper bounds) of different users are coupled with the function $f(\cdot)$. In contrast, by converting into such a QoS problem, they are decoupled to different constraints in the form of SINRs, which is helpful for the subsequent derivations. As these optimal SINRs are demanded, this reformulation, while does not directly help solve $\mathbf{P1}$, can help understand the structure of the optimal precoding vectors.

C. Optimal Solution Structure

Note that the constraint $\text{SINR}_k \geq \gamma_k$ always holds in the case of $\gamma_k = 0$ and clearly the corresponding solution is $\mathbf{p}_k = \mathbf{0}$, we conclude that the users with zero-rate can be eliminated from $\mathbf{P2}$. Consequently, we here assume $\gamma_k > 0$ without loss of generality.

The constraints can be transformed into the following tractable quadratic form

$$\text{SINR}_k \geq \gamma_k \Longleftrightarrow \mathcal{C}_k \leq 0, \forall k, \tag{13}$$

where the constraint function is defined as

$$\mathcal{C}_k \triangleq 1 + \sum_{i \neq k}^{K} \frac{1}{\sigma_n^2} \mathbf{p}_i^H \mathbf{R}_k \mathbf{p}_i - \frac{1}{\sigma_n^2 \gamma_k} \mathbf{p}_k^H \mathbf{R}_k \mathbf{p}_k. \tag{14}$$

The optimization problem can be reformulated as

$$\mathbf{P3}: \quad \min_{\mathbf{p}_1, \ldots, \mathbf{p}_K} \sum_{k=1}^{K} \mathbf{p}_k^H \mathbf{p}_k, \quad \text{s.t.} \quad \mathcal{C}_k \leq 0, \quad k = 1, \ldots, K. \tag{15}$$

The appropriate transformation lends itself to the analysis of the following solution structure.

The Lagrangian of $\mathbf{P3}$ can be expressed as

$$\mathcal{L}_{\mathcal{R}} = \sum_{k=1}^{K} \mathbf{p}_k^H \mathbf{p}_k + \sum_{k=1}^{K} \mu_k \mathcal{C}_k, \tag{16}$$

where μ_k is the Lagrange multiplier. The derivative of $\mathcal{L}_{\mathcal{R}}$ can be written as

$$\frac{\partial \mathcal{L}_{\mathcal{R}}}{\partial \mathbf{p}_k} = \mathbf{p}_k + \sum_{i \neq k}^{K} \frac{\mu_i}{\sigma_n^2} \mathbf{R}_i \mathbf{p}_k - \frac{\mu_k}{\sigma_n^2 \gamma_k} \mathbf{R}_k \mathbf{p}_k. \tag{17}$$

Denote that $\boldsymbol{\mu} = [\mu_1 \ \mu_2 \ \ldots \ \mu_K]^T \in \mathbb{C}^{K \times 1}$. The optimal solution of $\mathbf{P3}$ should satisfy the following Karush-Kuhn-Tucker (KKT) conditions

$$\frac{\partial \mathcal{L}_{\mathcal{R}}}{\partial \mathbf{p}_k}(\boldsymbol{\mu}, \mathbf{p}_k) = 0, \quad k = 1, \ldots, K, \tag{18}$$

$$\mu_k \mathcal{C}_k = 0, \quad k = 1, \ldots, K, \tag{19}$$

$$\mu_k \geq 0, \quad k = 1, \ldots, K. \tag{20}$$

Denote $\mathbf{p}_k = \sqrt{\rho_k} \underline{\mathbf{p}}_k$, where ρ_k is the power parameter of the k-th user, $\underline{\mathbf{p}}_k$ is the normalized precoding vector satisfying $\underline{\mathbf{p}}_k^H \underline{\mathbf{p}}_k = 1$. Note that even if the constraints are non-convex, the KKT condition is still a necessary condition for the optimal solution [45]. According to the above derivation, we can investigate the precoding characteristics in the following.

1) Generalized Eigen Domain Precoding: According to (18), we can obtain

$$\mu_k \mathbf{R}_k \underline{\mathbf{p}}_k = \gamma_k \Big(\sigma_n^2 \mathbf{I} + \sum_{i \neq k}^{K} \mu_i \mathbf{R}_i\Big) \underline{\mathbf{p}}_k. \tag{21}$$

This article has been accepted for publication in a future issue of this journal, but has not been fully edited. Content may change prior to final publication. Citation information: DOI 10.1109/TCOMM.2021.3105569, IEEE Transactions on Communications

This is a well-known generalized eigenvalue problem. According to (4), the covariance matrices can be computed by

$$\mathbf{R}_k = \beta_k^2 \bar{\mathbf{h}}_k \bar{\mathbf{h}}_k^H + (1-\beta_k^2)\mathbf{V}_{M_t}\mathbf{\Lambda}_k\mathbf{V}_{M_t}^H, \tag{22}$$

where $\mathbf{\Lambda}_k \in \mathbb{C}^{NM_t \times NM_t}$ is diagonal with $[\mathbf{\Lambda}_k]_{ii} = [\boldsymbol{\omega}_k]_i, \forall i$. The computation of μ_k will be discussed in the next section. Denote

$$\mathbf{S}_k = \mu_k \mathbf{R}_k, \tag{23}$$

and

$$\mathbf{N}_k = \sigma_n^2 \mathbf{I} + \sum_{i \neq k}^{K} \mu_i \mathbf{R}_i, \tag{24}$$

then $\underline{\mathbf{p}}_k$ is the generalized eigenvector with respect to generalized eigenvalue γ_k of matrix pair $(\mathbf{S}_k, \mathbf{N}_k)$. Although γ_k's are unknown, it is not necessary to compute them in advance due to the following theorem, proved in Appendix B.

Theorem 1: The optimal solution of $\mathbf{P3}$ is the generalized eigenvector with respect to the maximum generalized eigenvalue of matrix pair $(\mathbf{S}_k, \mathbf{N}_k)$, i.e.,

$$\underline{\mathbf{p}}_k = \max .\text{generalized eigenvector}(\mathbf{S}_k, \mathbf{N}_k), \tag{25a}$$

$$\gamma_k = \max .\text{generalized eigenvalue}(\mathbf{S}_k, \mathbf{N}_k). \tag{25b}$$

Theorem 1 indicates that once the Lagrange multipliers are determined, the precoding direction $\underline{\mathbf{p}}_k$ can be computed immediately. The key of the precoder is the introduction of the Lagrange multipliers, which is conducive to reduce the dimension of the problem. As the optimal Lagrange multipliers are implicit, we propose to compute them by deep neural networks in Section IV-B. The γ_k's also play a crucial role in computing the power parameters, as discussed in Section III-C2. Although $\mathbf{P3}$ is parameterized by the solution to $\mathbf{P1}$, i.e., $\{\gamma_k\}$, these SINRs can also be computed by $\{\mu_k\}$ and unnecessary to be obtained in advance.

It is worth pointing out that the structure in [36] is dedicated to the vector channel with the rank of covariance matrix being 1. Our proposed structure covers the general case with arbitrary rank. Note that the structure in [36] can be regarded as a special case of (25a), so are some other existing methods, which implies the universality of the proposed structure. Below we give the brief analyses.

Remark 1: From [5], [46], we can accordingly define the SLNR of the k-th user with an imperfect channel as

$$\text{SLNR}_k = \frac{\mathbf{p}_k^H \mathbf{R}_k \mathbf{p}_k}{\sigma_n^2 + \sum_{i \neq k}^{K} \mathbf{p}_k^H \mathbf{R}_i \mathbf{p}_k}. \tag{26}$$

As the precoder is decoupled from the users and independent of the allocated powers, the SLNR precoder usually considers equal power allocation [47], [48], and the robust SLNR precoder is

$$\underline{\mathbf{p}}_k = \max .\text{generalized eigenvector}(\mathbf{R}_k, \frac{K\sigma_n^2}{P}\mathbf{I} + \sum_{i \neq k}^{K} \mathbf{R}_i). \tag{27}$$

If we set $\mu_k = \frac{P}{K}, \forall k$, (25a) boils down to (27), which is the optimal precoder that maximizes SLNR. In this sense, (25a) can be regarded as the weighted SLNR precoder.

Remark 2: When $\beta_k = 1, \forall k$, (21) turns to the structure in [36]

$$\underline{\mathbf{p}}_k = \xi_k \mu_k \big(\sigma_n^2 \mathbf{I} + \sum\nolimits_{i=1}^{K} \mu_i \bar{\mathbf{h}}_i \bar{\mathbf{h}}_i^H\big)^{-1} \bar{\mathbf{h}}_k, \tag{28}$$

where $\xi_k = (1 + \frac{1}{\gamma_k})\bar{\mathbf{h}}_k^H \underline{\mathbf{p}}_k$. Similarly, if we set $\mu_k = \frac{P}{K}, \forall k$, it becomes the RZF precoder. By introducing the Lagrange multipliers, the performance of the RZF precoder can be immediately improved to WMMSE precoder.

Remark 3: When $\beta_k = 0, \forall k$, we have $\mathbf{R}_k = \mathbf{V}_{M_t}\mathbf{\Lambda}_k\mathbf{V}_{M_t}^H$. If we set $N_h = N_v = 1$, then $\mathbf{V}_{M_t}^H \mathbf{V}_{M_t} = \mathbf{I}_{M_t}$, (21) becomes

$$\mu_k \mathbf{\Lambda}_k \underline{\mathbf{q}}_k = \gamma_k \big(\sigma_n^2 \mathbf{I} + \sum_{i \neq k} \mu_i \mathbf{\Lambda}_i\big)\underline{\mathbf{q}}_k \Longleftrightarrow \mathbf{\Xi}_k \underline{\mathbf{q}}_k = \gamma_k \underline{\mathbf{q}}_k, \tag{29}$$

where $\underline{\mathbf{q}}_k = \mathbf{V}_{M_t}^H \underline{\mathbf{p}}_k$ and $\mathbf{\Xi}_k$ is diagonal and with $[\mathbf{\Xi}_k]_{ii} = [\mu_k \big(\sigma_n^2 \mathbf{I} + \sum_{i \neq k} \mu_i \mathbf{\Lambda}_i\big)^{-1} \mathbf{\Lambda}_k]_{ii}$. Denote $m_k = \arg\max_i [\mathbf{\Xi}_k]_{ii}$ the index of the maximum diagonal element, we have

$$[\underline{\mathbf{q}}_k]_i = \begin{cases} 1, & \text{if } i = m_k, \\ 0, & \text{otherwise.} \end{cases} \tag{30}$$

As such, the precoding vector $\underline{\mathbf{p}}_k = \mathbf{V}_{M_t}\underline{\mathbf{q}}_k$ is the m_k-th column of $\mathbf{V}_{M_t}$. In this sense, (25a) can be regarded as an extension of beam division multiple access (BDMA) transmission [49] and the introduction of the Lagrange multipliers provides a criterion of beam selection.

Note that the generalized eigenvector only contains the precoding direction information. The power parameters ρ_k can be computed by another KKT condition, which will be discussed below.

2) Generalized Eigen Domain Power Control: As has been proved in Appendix A, the constraint of the optimal solution in $\mathbf{P2}$ takes the equal sign, i.e., $\mathcal{C}_k = 0$. Thus, we have

$$\sigma_n^2 + \sum_{i \neq k}^{K} \underline{\mathbf{p}}_i^H \mathbf{R}_k \underline{\mathbf{p}}_i \cdot \rho_i - \frac{1}{\gamma_k} \underline{\mathbf{p}}_k^H \mathbf{R}_k \underline{\mathbf{p}}_k \cdot \rho_k = 0. \tag{31}$$

Denote

$$t_{ki} = \begin{cases} \frac{1}{\gamma_k} \underline{\mathbf{p}}_i^H \mathbf{R}_k \underline{\mathbf{p}}_i, & k = i, \\ -\underline{\mathbf{p}}_i^H \mathbf{R}_k \underline{\mathbf{p}}_i, & k \neq i. \end{cases} \tag{32}$$

We can rewritten (31) as

$$\sum_{i=1}^{K} t_{ki} \rho_i = \sigma_n^2, \quad k = 1, \ldots, K, \tag{33}$$

the matrix form of which is $\mathbf{T}\boldsymbol{\rho} = \sigma_n^2 \mathbf{1}_{K \times 1}$, where $[\mathbf{T}]_{ki} = t_{ki}$ and $\boldsymbol{\rho} = [\rho_1 \ \rho_2 \ \ldots \ \rho_K]^T$. To compute the power vector $\boldsymbol{\rho}$, we first propose the following lemma, proved in Appendix C.

Lemma 2: The matrix $\mathbf{T}$ is non-singular.

Thus, the power vector can be computed by

$$\boldsymbol{\rho} = \sigma_n^2 \mathbf{T}^{-1} \mathbf{1}_{K \times 1}. \tag{34}$$

It is worth mentioning that the precoding vectors computed by the solution structure, i.e., (25a) and (34), always satisfy the total power constraint as the optimal Lagrange multipliers satisfy (proved in Appendix B)

$$\sum\nolimits_{k=1}^{K} \rho_k = \sum\nolimits_{k=1}^{K} \mu_k \leq P. \tag{35}$$

The power parameters cannot be determined directly as the γ_k's are unknown. However, it can be connected with the Lagrange multipliers thanks to Theorem 1. Beyond the precoding direction, the Lagrange multipliers also determine the γ_k's, which further determine the power parameters.

IV. Robust Precoder Design Based on Neural Networks

Note that $\mathbf{P2}$ and $\mathbf{P3}$ are only used to assist in deriving the solution structure; it is unnecessary to be solved. Based on the previous analysis, we conclude that the precoding vectors can be generated losslessly by the Lagrange multipliers. The precoding direction can be computed by solving the generalized eigenvalue problem in (21), and the power parameters can be further computed by the closed-form expression in (34). As such, the high-dimensional computation of the precoding vectors turns into low-dimensional Lagrange multipliers, i.e., the key to downlink precoder design. Learning the precoding vectors directly is complicated and difficult to train due to the high dimension of precoding vectors. However, learning the Lagrange multipliers has no such limitation as the dimension has been much reduced. In this section, we will propose a general framework for robust precoder design by taking advantage of this optimal solution structure, where the Lagrange multipliers are computed by a well-trained neural network.

A. Framework Structure

The following theorem, proved in Appendix D, provides the physical meaning of the Lagrange multipliers.

Theorem 2: Denote $(\mu_1^\diamond, \ldots, \mu_K^\diamond)$ the optimal solution of the following optimization problem, $\mathbf{P4}$, then the precoding vectors constructed by the structure in (25a) and (34) using $\{\mu_k^\diamond\}$ is the optimal solution of $\mathbf{P1}$.

$$\mathbf{P4}: \quad \max_{\mu_1,\ldots,\mu_K} f(\check{\mathcal{R}}_1, \ldots, \check{\mathcal{R}}_K), \quad \text{s.t.} \ \sum_{k=1}^{K} \mu_k \le P, \tag{36}$$

where $\check{\mathcal{R}}_k = \log\Big(1 + \rho\big(\mathbf{N}_k^{-1}\mathbf{S}_k\big)\Big)$ and $\rho(\cdot)$ denotes the function of the maximum eigenvalue.

Theorem 2 establishes a relationship between the solutions of $\mathbf{P1}$ and $\mathbf{P4}$. Given a feasible solution of $\mathbf{P4}$, the precoding vectors constructed by the structure in (25a) and (34) are a feasible solution of $\mathbf{P1}$, whose objective is equal to that of $\mathbf{P4}$. When the solution of $\mathbf{P4}$ is globally optimal, then the corresponding constructed precoder is also globally optimal for $\mathbf{P1}$.

Remark 4: If we set $\beta_k = 1, \forall k$, as the rank of matrix $\mathbf{N}_k^{-1}\mathbf{S}_k$ is 1, we have

$$\check{\mathcal{R}}_k = \log\det(\sigma_n^2\mathbf{I} + \sum_{i=1}^{K}\mu_i\mathbf{R}_i) - \log\det(\sigma_n^2\mathbf{I} + \sum_{i\neq k}^{K}\mu_i\mathbf{R}_i). \tag{37}$$

As such, the Lagrange multipliers can be regarded as the uplink power parameters, and $\mathbf{P4}$ can be regarded as the power allocation. For sum rate maximization, it can be solved by the WMMSE approach [50].

However, for the general case, there is no closed-form exact solution available in the literature to solve $\mathbf{P4}$ directly. The existing algorithms, e.g., augmented Lagrangian method, are numerical iterative. On the contrary, once the neural network is well-trained, the Lagrange multipliers can be immediately computed without resorting to the iteration. The training process is offline to reduce online computation, which is one of the advantages of deep learning for wireless communications. Further, once the Lagrange multipliers are computed, the precoding vectors can be immediately computed without resorting to the iterative algorithms in [17], which significantly reduce the complexity (see Sec. VI).

The general framework for robust precoder design can be decomposed into three parts:

i) Learn the optimal Lagrange multipliers from the obtained channel vectors;
ii) Compute precoding direction by solving a generalized eigenvalue problem;
iii) Compute power parameters by a closed-form expression in (34).

The corresponding algorithm is summarized in Algorithm 1. Noting that $\mathbf{p}_k = \mathbf{0}$ if $\mu_k = 0$, as there exist slight errors of the neural network, we delete the k-th user if $\mu_k \le \epsilon$, where ϵ is a preset threshold.

Algorithm 1 General Framework for Robust Precoder Design

Input: The channel vectors $\bar{\mathbf{h}}_k$, $\boldsymbol{\omega}_k$, the noise variance σ_n and total power constraint P
Output: The precoding vectors $\mathbf{p}_k, k = 1, \ldots, K$
1: Compute the corresponding parameters $\beta_k, k = 1, \ldots, K$.
2: Compute the corresponding Lagrange multipliers $\mu_k, k = 1, \ldots, K$ and delete users with $\mu_k \le \epsilon$.
3: Compute the normalized precoding vector $\underline{\mathbf{p}}_k$ and the parameter $\gamma_k, k = 1, \ldots, K$ by (25a).
4: Compute the power allocated on the users $\rho_k, k = 1, \ldots, K$ by (34).
5: Compute the precoding vectors $\mathbf{p}_k = \sqrt{\rho_k}\underline{\mathbf{p}}_k, k = 1, \ldots, K$.

B. Lagrange Multiplier Neural Network

The excellent representation ability of the neural network, such as the function (mapping) approximation, is beyond the traditional method. Besides, thanks to its generalization ability, it can be deployed in different wireless scenarios while the traditional method needs to be re-optimized when the environment or parameters change.

The objective is to approximate Lagrange multipliers from channel vectors. According to the posteriori model, denote

$$\bar{\mathbf{H}}_{\boldsymbol{\beta}} = [\beta_1\bar{\mathbf{h}}_1, \ldots, \beta_K\bar{\mathbf{h}}_K]^H \in \mathbb{C}^{K\times M_t}, \tag{38}$$

$$\boldsymbol{\Omega}_{\boldsymbol{\beta}} = [(1-\beta_1^2)\boldsymbol{\omega}_1, \ldots, (1-\beta_k^2)\boldsymbol{\omega}_K]^H \in \mathbb{C}^{K\times NM_t}, \tag{39}$$

as the input of the neural network. As $\mathbf{V}_{M_t}$ is constructed from the oversampling DFT matrices, $\boldsymbol{\omega}_k$ is generally sparse. Besides, the CSI contains two-dimensional information. Both of the characteristics can be taken advantages by convolutional neural network (CNN) [51]. The CNNs have been widely-adopted for feature extraction from CSI [52], [53]. Although these features are recessive, simulations and practical applications have proven its effectiveness. Compared with fully connected, the convolutional neural networks can reduce the

number of learned parameters by parameter sharing. Moreover, the pooling adopted in CNN can reduce the dimensionality of the input data, which means the computational complexity of the network can be reduced. For these considerations, we utilize CNN to learn the Lagrange multipliers.

The convolutional neural network is composed of several convolution modules, a flatten layer and several fully-connected layers. Each convolution module consists of a convolutional layer, an activation function and a pooling layer. The convolutional layer performs convolutions on the input to extract the feature. Besides, the max-pooling is chosen for down-sampling and the widely-adopted rectified linear unit (ReLU) (i.e., $h(x) = \max(0, x)$) is chosen as an activation function, which removes negative values to increase nonlinearity. Next, the flatten layer transforms the feature into a suitable form (i.e., a vector) for the next layers. Finally, the fully-connected layers accomplish the advanced reasoning by matrix multiplications, where the activation function is also chosen as ReLU. The Lagrange multipliers are also related to the total power constraint P and noise covariance σ_n^2, which determines the signal-to-noise ratio (SNR) at the transmitter

$$\nu = 10 \lg \frac{P}{\sigma_n^2}. \tag{40}$$

It can be included in the channel vectors, however, may cause great fluctuations in the order of magnitude of the input value under samples with different constraints.

As such, we construct the neural network consisting of a CNN and a fully-connected neural network (FNN), as shown in Fig. 2. The former encodes the channel vectors as the implicit feature, and the latter decodes the feature with SNRs as the Lagrange multipliers. The channel matrix, $\bar{\mathbf{H}}_{\boldsymbol{\beta}}$, is divided into the real and imaginary parts. The Lagrange multipliers learning can be decomposed into two steps:

1) *Encoder*: Several convolution modules to encode the CSI as hidden layer feature $\boldsymbol{\kappa} = f_{en}(\bar{\mathbf{H}}_{\boldsymbol{\beta}}, \boldsymbol{\Omega}_{\boldsymbol{\beta}}; \mathbf{w}_{en})$, where $\mathbf{w}_{en}$ denotes the weight vector of the encoder.
2) *Decoder*: Several fully-connected layers to decode the hidden layer feature $\boldsymbol{\kappa}$ and the SNR ν as the Lagrange multipliers $\boldsymbol{\mu} = f_{de}(\nu, \boldsymbol{\kappa}; \mathbf{w}_{de})$, where $\mathbf{w}_{de}$ denotes the weights vector of the decoder.

Thus, the function of Lagrange Multipliers Neural Network can be written in the form

$$\boldsymbol{\mu} = f_{\boldsymbol{\mu}}(\bar{\mathbf{H}}_{\boldsymbol{\beta}}, \boldsymbol{\Omega}_{\boldsymbol{\beta}}, \nu; \mathbf{w}), \tag{41}$$

where the set of all weight and bias parameters have been grouped together into a vector $\mathbf{w}$.

C. Dataset Generation and Neural Network Training

It has been proved that the precoding vectors can be computed by Lagrange multipliers, and interestingly vice versa. Thus, given the channel vectors, we propose to compute the Lagrange multipliers from precoding vectors by the existing iterative method. Left-multiplied by $\underline{\mathbf{p}}_k^H$, (21) becomes

$$\frac{1}{\gamma_k} \underline{\mathbf{p}}_k^H \mathbf{R}_k \underline{\mathbf{p}}_k \cdot \mu_k - \sum_{i \neq k}^{K} \underline{\mathbf{p}}_k^H \mathbf{R}_i \underline{\mathbf{p}}_k \cdot \mu_i = \sigma_n^2. \tag{42}$$

Algorithm 2 Dataset Generation

Input: The number of data samples $N_{\mathcal{D}}$
Output: The dataset $\mathcal{D}$
1: Initialize $i = 1$.
2: **while** $i < N_{\mathcal{D}}$ **do**
3: Generate the channel vectors $\bar{\mathbf{h}}_k^{(i)}$ and $\boldsymbol{\omega}_k^{(i)}$, the noise variance $\sigma_n^{(i)}$ and total power constraint $P^{(i)}$, compute the coefficient $\beta_k^{(i)}, k = 1, \ldots, K$ and the SNR $\nu^{(i)}$.
4: Solve the problem (10) by the iterative approach in (46), compute the precoding vectors $\mathbf{p}_k^{(i)}$ and the corresponding parameter $\gamma_k^{(i)}, k = 1, \ldots, K$.
5: Construct the matrix $\mathbf{T}^{(i)}$ by (32) and compute the corresponding Lagrange multipliers $\mu_k^{(i)}, k = 1, \ldots, K$ by (44).
6: Group $\beta_k^{(i)}$, $\bar{\mathbf{h}}_k^{(i)}$, $\boldsymbol{\omega}_k^{(i)}$, $\nu^{(i)}$ and $\mu_k^{(i)}, k = 1, \ldots, K$ as the i-th sample.
7: Set $i = i + 1$.
8: **end while**

We can rewritten (42) as

$$\sum_{i=1}^{K} t_{ik} \mu_i = \sigma_n^2, \quad k = 1, \ldots, K, \tag{43}$$

the matrix form of which is $\mathbf{T}^H \boldsymbol{\mu} = \sigma_n^2 \mathbf{1}_{K \times 1}$. As matrix $\mathbf{T}$ is non-singular, we can compute the Lagrange multipliers vector by

$$\boldsymbol{\mu} = \sigma_n^2 (\mathbf{T}^{-1})^H \mathbf{1}_{K \times 1}. \tag{44}$$

In this paper, we consider the sum rate maximization as an example

$$f(\mathcal{R}_1, \ldots, \mathcal{R}_K) = \mathcal{R}_{sum} = \sum\nolimits_{k=1}^{K} \mathcal{R}_k. \tag{45}$$

The precoding vectors can be computed by the following iterative equations [17]

$$\lambda^t \leftarrow \sum_{k=1}^{K} \mathrm{tr}\left(\left(\mathbf{p}_k^t\right)^H \left(\mathbf{A}_k^t - \mathbf{B}^t\right) \mathbf{p}_k^t \right), \tag{46a}$$

$$\mathbf{p}_k^{t+1} \leftarrow \left(\mathbf{B}^t + \lambda^t \mathbf{I}_{M_t}\right)^{-1} \mathbf{A}_k^t \mathbf{p}_k^t, \tag{46b}$$

where t denotes the number of iterations, $\mathbf{A}_k = (\sigma_n^2 + \sum_{i \neq k}^{K} \mathbf{p}_i^H \mathbf{R}_k \mathbf{p}_i)^{-1} \mathbf{R}_k$ and $\mathbf{B} = \sum_{k=1}^{K} \left(\mathbf{A}_k - (\sigma_n^2 + \sum_{i=1}^{K} \mathbf{p}_i^H \mathbf{R}_k \mathbf{p}_i)^{-1} \mathbf{R}_k \right)$.

In the offline stage, we compute the precoding vectors in advance by the above iterative approach and then obtain the Lagrange multipliers. Thus, the dataset can be generated, and the neural network can be trained. In the online stage, we can directly obtain the Lagrange multipliers by the well-trained neural network without knowing the precoding vectors in advance.

The dataset generation is illustrated in Algorithm 2. As the training is offline, the precoding vectors can be computed by the high-performance iterative approach without considering much complexity. In such a case, a sufficiently large enough number of iterations can be set until convergence. Furthermore, we can select multiple initial values to iterate and choose the best one to avoid some bad local optimal solutions. The dataset contains a large number of samples of different channel environments and qualities; therefore, the neural network can generalize well in unseen data and work for practical channels. For practical systems, the trained neural network can be

This article has been accepted for publication in a future issue of this journal, but has not been fully edited. Content may change prior to final publication. Citation information: DOI 10.1109/TCOMM.2021.3105569, IEEE Transactions on Communications

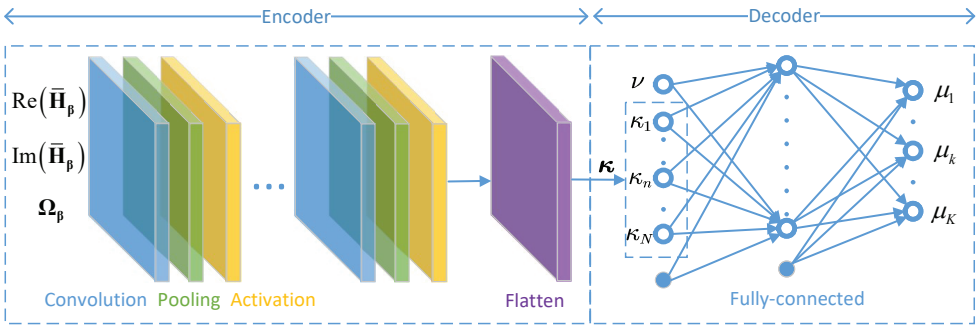

Fig. 2. The proposed neural network for Lagrange multipliers learning.

directly applied to each time slot without retraining. We only need to take the CSI of the current block as the input of the neural network to get the desired Lagrange multipliers. The channel samples are not limited to be generated by channel models but also can be practical measurements. Note that the training is offline; therefore, the neural network can be applied for online communication systems without training overhead.

Given the training set $\mathcal{D}$ generated by Algorithm 2, the objective is to minimize the loss function

$$\mathcal{L}_{\mathcal{D}} = \frac{1}{N_{\mathcal{D}}} \sum_{i=1}^{N_{\mathcal{D}}} \left\| \boldsymbol{\mu}^{(i)} - \hat{\boldsymbol{\mu}}^{(i)} \right\|^2, \tag{47}$$

where $\hat{\boldsymbol{\mu}}^{(i)}$ is the predicted results of the i-th sample. In the training progress, the procedure of dropout is utilized to avoid over-fitting. Finally, we employ the widely-used adaptive moment estimation (ADAM) algorithm to train the neural network and weights vector $\mathbf{w}$ can be obtained.

V. Low-complexity Weighting Framework

The proposed general precoding framework based on the neural network can achieve near-optimal performance, and the complexity has been significantly reduced compared with the existing iterative algorithm. However, further simplified computation is desired to be applied in a real-time system. To this end, we further propose a low-complexity framework in this section.

A. Weighting Strategy for Robust Precoder

The complexity is mainly in the following three parts:

1) The neural network for the Lagrange multipliers;
2) The generalized eigenvalue problem for the precoding direction;
3) The computation of the power parameters (including the construction of matrix $\mathbf{T}$).

When only instantaneous CSI is available, the computational complexity can be much simplified by utilizing mathematical manipulation (e.g., matrix inversion lemma). When only statistical CSI is used, only once the computation is required as it remains unchanged for the whole period of time-frequency resources. Thus, it is an efficient strategy to decompose the general framework into instantaneous and statistical parts. As the Lagrange multipliers should still satisfy $\sum_{k=1}^{K} \mu_k = P$, we compute the Lagrange multipliers as

$$\mu_k = \beta_k^2 [\boldsymbol{\mu}_{\mathbf{h}}]_k + (1 - \beta_k^2)[\boldsymbol{\mu}_{\boldsymbol{\omega}}]_k, \tag{48}$$

where $\boldsymbol{\mu}_{\mathbf{h}}$ and $\boldsymbol{\mu}_{\boldsymbol{\omega}}$ denote the Lagrange multipliers of the two extremes, respectively. As the construction of matrix $\mathbf{T}$ is also time-consuming, we weight the powers with the same strategy. The power parameters can be computed as

$$\rho_k = \beta_k^2 [\boldsymbol{\rho}_{\mathbf{h}}]_k + (1 - \beta_k^2)[\boldsymbol{\rho}_{\boldsymbol{\omega}}]_k, \tag{49}$$

where $\boldsymbol{\rho}_{\mathbf{h}}$ and $\boldsymbol{\rho}_{\boldsymbol{\omega}}$ denote the power of the two extremes.

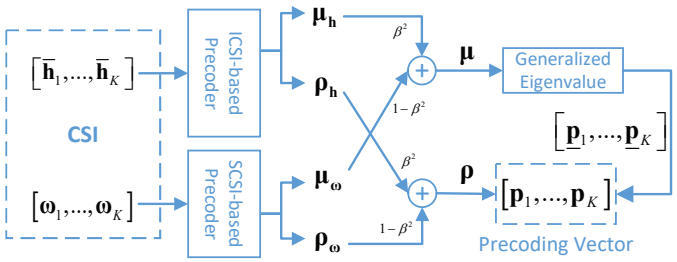

Fig. 3. Low-complexity Framework for Robust Precoder Design.

The low-complexity framework is shown in Fig. 3. As the Lagrange multipliers and the power parameters can be computed efficiently by the weighting strategy, now we focus on the efficient computation of generalized eigenvalue problem. It can be solved by transforming it into a standard eigenvalue problem with the operation of matrix inversion. However, due to the high dimension, the matrix inversion is exactly what needs to be avoided. To solve the generalized eigenvalue problem with acceptable complexity, we have utilized the conjugate gradient (CG) methods [54], which approaches the minimum generalized eigenvalue by an iterative method. The algorithm of the low-complexity framework is illustrated in Algorithm 3.

To develop the low-complexity framework, we heuristically decomposing the original problem into computationally efficient sub-problems by the weighting strategy. Nonetheless, it provides a promising sum rate performance with low complexity, which will be confirmed by simulation results in Sec. VI. In the rest of this section, we will provide a detailed analysis of the precoder in the two extremes.

Algorithm 3 Low-complexity Framework for Robust Precoder Design

Input: The channel vectors $\bar{\mathbf{h}}_k$ and $\boldsymbol{\omega}_k$, the noise variance σ_n, and total power constraint P

Output: The precoding vectors $\hat{\mathbf{p}}_k, k = 1, \ldots, K$

1: Compute the corresponding parameters $\beta_k, k = 1, \ldots, K$.
2: Compute the Lagrange multipliers $\boldsymbol{\mu}_{\mathbf{h}}$ and the power parameters $\boldsymbol{\rho}_{\mathbf{h}}$ based on the instantaneous CSI.
3: Compute the Lagrange multipliers $\boldsymbol{\mu}_{\boldsymbol{\omega}}$ and the power parameters $\boldsymbol{\rho}_{\boldsymbol{\omega}}$ based on the statistical CSI.
4: Compute the Lagrange multipliers by (48) and the power parameters by (49). Delete users with $\mu_k \leq \epsilon$.
5: Compute the normalized precoding vector $\underline{\mathbf{p}}_k$ and the parameter $\gamma_k, k = 1, \ldots, K$ in (25a) by conjugate gradient method.
6: Compute the precoding vectors $\mathbf{p}_k = \sqrt{\rho_k}\underline{\mathbf{p}}_k, k = 1, \ldots, K$.

B. Instantaneous CSI-Based Precoder

As has been analyzed in IV-A, the Lagrange multipliers can be computed by the WMMSE approach when only instantaneous CSI is available. Besides, we can similarly train a neural network which takes $\bar{\mathbf{H}} = [\bar{\mathbf{h}}_1, \ldots, \bar{\mathbf{h}}_K] \in \mathbb{C}^{K \times M_t}$ as the input and $\boldsymbol{\mu}_{\mathbf{h}} \in \mathbb{C}^{K \times 1}$ as the output. However, due to the high dimension of channel vectors, the complexity of either WMMSE or neural network is not as low as expected. Thus, to further reduce the complexity without pursuing the optimal solution, the Lagrange multipliers can be computed by some suboptimal precoding vectors such as the RZF precoder.

C. Statistical CSI-Based Precoder

As analyzed before, only once the computation is required during the period of time-frequency resources. Thus, it is acceptable to compute the precoding vector by an iterative approach. However, in some specific communication systems, different subcarriers and slots may be assigned to different users, where the statistical CSI is not the same. To expand the scope of application, we propose to compute the statistical Lagrange multipliers by statistical CSI learning, which is similar to the strategy in the general framework. To be more specific, the Lagrange multipliers are computed by the neural networks, whose structure is similar to Fig. 3, the only difference is that the input is only statistical CSI. The detailed training progress can be seen in Section IV.

VI. Simulation Results

In this section, we present simulation results to evaluate the performance of the proposed approaches, using the QuaDRiGa channel model [55], which is a 3-D geometry-based stochastic model with time evolution. In particular, we consider a massive MIMO system consisting of one BS and $K = 40$ users. The BS is equipped with $M_t = 128$ antennas (UPA, $M_v = 8$, $M_h = 16$) and the height of BS is 25m. Users with single antenna are randomly distributed in the cell with radius r = 100m at 1.5m height. Each time slot takes up 0.5ms and consists of 10 blocks. The centre frequency is set at 4.8 GHz and the bandwidth is 20 MHZ. For the QuaDRiGa model, we consider the *3GPP_3D_UMa_NLOS* (urban macro) scenario [55] and utilize oversampling DFT matrix (oversampling factor $N_v = 2$, $N_h = 2$) to transform channels into the beam domain. Three mobile scenarios with moving speeds 30, 80 and 240 kmph, are considered. Since the channel correlation among different blocks decreases with increasing mobility, the moving speed is connected to the estimated channel correlation coefficient, $\beta_{k,m,n}$.

A. Neural Network Performance

The neural network structure and major parameters are shown in Table I. Considering that the dataset generation and neural network training is offline, on the balance of generalization performance and the consuming time, we choose the size of 160,000. The input of Lagrange multipliers neural network can be expressed as

$$\mathbf{X} = [\mathrm{Re}(\mathbf{H}_{\boldsymbol{\beta}}) \;\; \mathrm{Im}(\mathbf{H}_{\boldsymbol{\beta}}) \;\; \boldsymbol{\Omega}_{\boldsymbol{\beta}}]^H. \tag{50}$$

The dimension of input is and 768×40 and the size of extracted feature after four convolution modules is $1 \times 40 \times 2$, which can be flattened into a vector $\mathbf{m}$. Furthermore, group $\mathbf{m}$ and P into a 81×1 vector as the input of the fully-connected layers, the unit number of hidden layer is 1024, and the output is $\boldsymbol{\mu}$. The structure of the statistical Lagrange multipliers neural network is similar; the differences are that the input of convolution modules is $\boldsymbol{\Omega}_{\boldsymbol{\beta}}$ and the hyper-parameters are partially different. The other main parameters are shown on the right side of the table, which are shared by the two networks. The neural networks are trained by GeForce RTX 3080 GPU, and cost 276 minutes and 191 minutes, respectively.

As the dataset is generated offline, the computational complexity of the iterative approach is affordable. Thus, the number of iterations is set as $N_{iter} = 20$, which suffices to converge as observed in [17]. Besides, to enhance the generalization performance, various scenarios are considered in the dataset, e.g., different mobile velocities, SNRs, user distributions, etc. As such, the trained neural network can be applied to various practical scenarios. Once the neural network is well-trained, it can be used in real-time communication without training overhead, as it is unnecessary to be re-trained when the channel changes.

It is worth mentioning that the iterative algorithm achieves local optimal solutions by optimizing precoding vectors instead of the Lagrange multipliers to maximize the sum rate. Thus, the iterative approach with different initial values may achieve solutions with a similar sum rate, and the corresponding Lagrange multipliers may differ sometimes. Table II shows an example of the above situation, which means different local optimum Lagrange multipliers may achieve similar sum rate. To find a better one (if not global optimal), 10 different initial values are used, respectively, and the best one is chosen to be one sample for robustness against accidentally bad local optimal solutions.

To evaluate the performance of the proposed neural networks, we first simulate the upper bound of the ergodic rate. Fig. 4 (a) shows the sum rate upper bound of general framework versus SNR in various mobile scenarios. Since the data set is generated from the iterative approach in (46), we take it as a benchmark. As can be seen, the general framework achieves near-optimal performance in various mobile scenarios. Fig. 4 (b) shows the sum rate upper bound of low-

This article has been accepted for publication in a future issue of this journal, but has not been fully edited. Content may change prior to final publication. Citation information: DOI 10.1109/TCOMM.2021.3105569, IEEE Transactions on Communications

TABLE I
NEURAL NETWORK STRUCTURE AND MAJOR PARAMETERS

Lagrange Multipliers Neural Network (Input Size: 768×40)			Statistical Only (Input Size: 512×40)			Major Hyper-parameter	
Kernel Size (Num)	Pooling	Feature Size	kernel Size (Num)	Pooling	Feature Size	Dataset Size	160000
48×5 (4)	8×1	$96 \times 40 \times 4$	32×5 (4)	8×1	$64 \times 40 \times 4$	Batchsize	1024
24×5 (8)	6×1	$16 \times 40 \times 8$	16×5 (8)	4×1	$16 \times 40 \times 8$	Algorithm	ADMA
8×5 (4)	4×1	$4 \times 40 \times 4$	8×5 (4)	4×1	$4 \times 40 \times 4$	Learning Rate	0.001
4×5 (2)	4×1	$1 \times 40 \times 2$	4×5 (2)	4×1	$1 \times 40 \times 2$	Dropout	0.5
$81 - 1024 - 40$			$81 - 1024 - 40$			Training Steps	10000

TABLE II
AN EXAMPLE OF LAGRANGE MULTIPLIERS AND SUM RATE

Lagrange multipliers	sum rate (bit/s/Hz)
[0.3976, 0.5054, 0.4801, 0, 0.4821, ...]	221.9684
[0.6659, 0, 0, 0.8371, 0.6224, ...]	219.6985

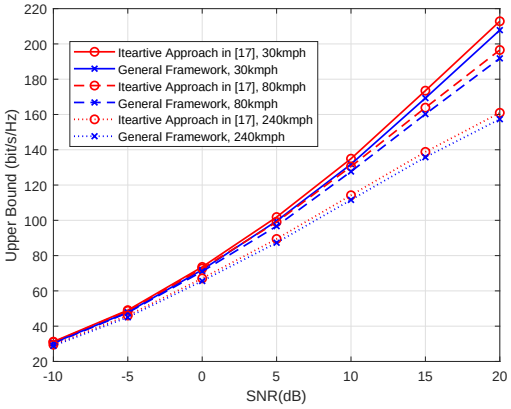

(a) General Framework

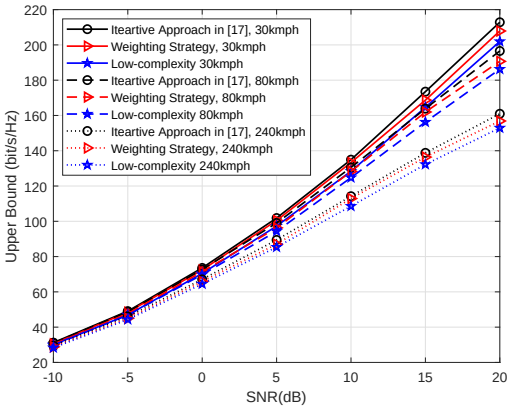

(b) Low-complexity Framework

Fig. 4. Sum rate upper bound of general and low-complexity frameworks versus SNR in various mobile scenarios.

complexity framework versus SNR in various mobile scenarios. The iterative approach and the weighting strategy with the optimal Lagrange multipliers (computed by the solution of iterative approach) are presented here as benchmarks to evaluate the loss of the weighting strategy and the neural network, respectively. There exists a little performance loss in the low-complexity framework due to the weighting operation. Besides, little gap between the optimal and approximated Lagrange multipliers implies that the neural network is robust to new scenarios not available in the training set as the training set, validation set, and testing set are separate.

To adapt to the wireless networks with a dynamic number of users, we design the neural network with fixed input size, where the dataset contains samples with different user configurations under the maximum number of users allowed in a cell. For the underload system, e.g., $K \leq 40$, the input dimension does not exceed this fixed value and the corresponding lack portion of its channel matrix is set to be zero; the proposed neural network can automatically output the desired solution. For the overload system, e.g., $K > 40$, user selection should be applied before applying the neural network. In addition, the work in [56] uses transfer learning to address this kind of issues. Another possibility to deal with the varying number of users is to employ graph neural network as in [57]. This is a very interesting topic to be investigated in the future work.

B. Sum Rate Performance of Proposed Frameworks

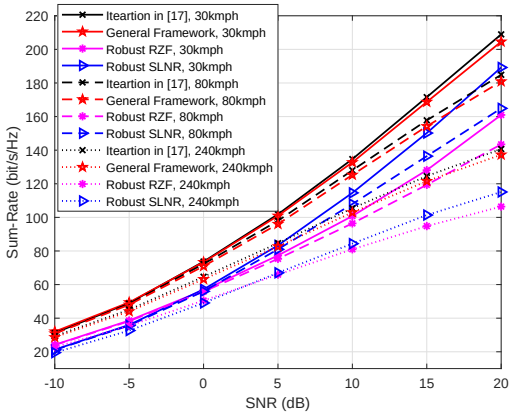

Fig. 5. Sum rate versus SNR with respect to different precoding approaches.

We first simulate the sum rate to evaluate the performance of the proposed general frameworks. Fig. 5 shows the sum rate versus SNR with respect to different precoding approaches. Compared with Fig. 4, we have that the upper bound is tight to the ergodic rate. The robust RZF precoder in [58] and the robust SLNR precoder in (27) are presented here as a baseline. As can be seen, the robust RZF precoder works well in the

This article has been accepted for publication in a future issue of this journal, but has not been fully edited. Content may change prior to final publication. Citation information: DOI 10.1109/TCOMM.2021.3105569, IEEE Transactions on Communications

low-mobility scenario and deteriorates as the mobile velocity increases. Besides, the SLNR precoder works slightly better than RZF. However, the gap between the SLNR precoder and the proposed frameworks grows with the increasing speed. In the case of 240 kmph at 20 dB, there exists about 19.3% and 29.0% gains of the sum rate in the general framework compared with the robust SLNR and the robust RZF precoders, respectively. As the robust SLNR precoder is a special case of the proposed structure, this gain implies that the precoding vectors are sensitive over the Lagrange multipliers. It is not surprising that the performance of the robust RZF and the robust SLNR precoders are unsatisfactory as both of them do not directly maximize the sum rate. The results show the improved performance of the proposed frameworks, especially in high-mobility scenarios.

We further simulate the sum rate to evaluate the performance of the proposed low-complexity frameworks. As can be seen in Fig. 6, the sum rate performance is unsatisfactory when only the ICSI-based or SCSI-based precoder. The former will be obsolete in high-mobility scenarios while the latter ignores channel estimates. By a weighting strategy, the low-complexity framework integrates the instantaneous or statistical Lagrange multipliers to achieve the robustness. In the case of 240 kmph at 20 dB, there exists about 29.5% gain on the sum rate in the low-complexity framework compared with the ICSI-based precoder.

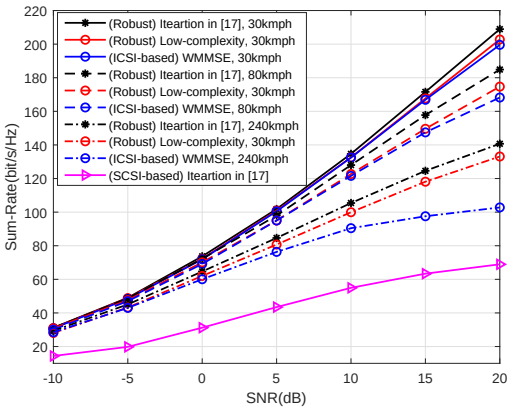

Fig. 6. Sum rate versus SNR with respect to different precoding approaches.

Table III illustrates the complexity of different precoding approaches. The typical numbers for multiplication operations are given, where parameters are set so that the performance of the corresponding algorithm is asymptotically optimal. Here we employ the CG method to reduce the complexity of the matrix inversion operation. Compared with the existing iterative approach in [17] for sum rate maximization, the general framework significantly reduces complexity while maintaining the near-optimal sum rate performance. The low-complexity framework further reduces the complexity with negligible performance loss. Compared with the robust SLNR precoder, it improves 15.6% sum rate with almost the same complexity. The robust RZF can achieve relatively low complexity; however, at the cost of degraded performance.

VII. Conclusion

In this paper, we have proposed a deep learning approach for downlink precoder design in massive MIMO, making use of channel estimates and statistical parameters of channel estimation error simultaneously. By transforming the original maximization problem into a QoS one, the optimal solution structure is characterized. With a Lagrangian formulation, the precoding directions and powers can be computed by solving a generalized eigenvalue problem that relies only on available CSI and the Lagrange multipliers. As such, the high-dimensional precoder design can be alternatively done by low-dimensional Lagrange multipliers, which can be computed by a learning approach. To further reduce the computational complexity, we decompose each Lagrange multiplier into two parts, corresponding to instantaneous and statistical CSI, respectively, so that these two parts can be learned separately with reduced complexity. It is observed from simulation results that the general framework achieves the near-optimal performance and the low-complexity framework significantly reduces the computational complexity but with negligible performance degradation.

Appendix A
Proof of Lemma 1

Denote $\mathbf{p}_k = \sqrt{\rho_k}\underline{\mathbf{p}}_k$, where ρ_k is the power allocated to the k-th user, $\underline{\mathbf{p}}_k$ is normalized precoding vector satisfying $\underline{\mathbf{p}}_k^H \underline{\mathbf{p}}_k = 1$. The SINR of k-th user can be rewritten as

$$\mathrm{SINR}_k = \frac{\rho_k \underline{\mathbf{p}}_k^H \mathbf{R}_k \underline{\mathbf{p}}_k}{\sigma_n^2 + \sum_{i\neq k}^K \rho_i \underline{\mathbf{p}}_i^H \mathbf{R}_k \underline{\mathbf{p}}_i}. \tag{51}$$

Then $\mathbf{P2}$ can be rewritten as

$$\begin{aligned} \min_{\rho_1,\ldots,\rho_K,\underline{\mathbf{p}}_1,\ldots,\underline{\mathbf{p}}_k} \quad & \sum_{k=1}^K \rho_k, \\ \text{s.t.} \quad & \mathrm{SINR}_k \geq \gamma_k, \\ & \underline{\mathbf{p}}_k^H \underline{\mathbf{p}}_k = 1, \end{aligned} \tag{52}$$

whose optimal solution and corresponding SINRs are denoted by $(\rho_1^\diamond, ..., \rho_K^\diamond, \underline{\mathbf{p}}_1^\diamond, ..., \underline{\mathbf{p}}_K^\diamond)$ and $\gamma_1^\diamond, \ldots, \gamma_K^\diamond$, respectively.

Owing to the constraints $\mathrm{SINR}_k \geq \gamma_k, \forall k$, assume there exists $\gamma_m^\diamond$ satisfying

$$\gamma_m^\diamond > \gamma_m. \tag{53}$$

It is easy to verify that SINR_k monotonically increases with the power allocated to itself ρ_k and decreases with the power allocated to other user $\rho_i, i \neq k$. As SINR_k is continuous with respect to ρ_m, there always exists a sufficiently small ε to establish a solution $(\rho_1^\diamond, ..., \rho_m^\diamond - \varepsilon, ..., \rho_K^\diamond, \underline{\mathbf{p}}_1^\diamond, ..., \underline{\mathbf{p}}_K^\diamond)$ whose corresponding SINRs $\gamma_1^\star, \ldots, \gamma_K^\star$ satisfy

$$\gamma_k^\star = \begin{cases} \gamma_k^\diamond - \varepsilon_k > \gamma_k, & k = m \\ \gamma_k^\diamond + \varepsilon_k > \gamma_k, & k \neq m \end{cases}, \tag{54}$$

where variables $\varepsilon_k > 0$ are sufficiently small. Thus, the solution $(\rho_1^\diamond, ..., \rho_m^\diamond - \varepsilon, ..., \rho_K^\diamond, \underline{\mathbf{p}}_1^\diamond, ..., \underline{\mathbf{p}}_K^\diamond)$ satisfies the constraint and achieves lower objective, simultaneously. This is contrary to that $(\rho_1^\diamond, ..., \rho_K^\diamond, \underline{\mathbf{p}}_1^\diamond, ..., \underline{\mathbf{p}}_K^\diamond)$ is the optimal solution. As a result, we can obtain that (53) does not hold and

$$\gamma_m^\diamond = \gamma_m, \tag{55}$$

TABLE III
COMPARISON OF COMPLEXITY AMONG DIFFERENT PRECODING APPROACHES

Algorithm	Complexity	Typical Value	Denotation
Iterative Approach [17]	$O\left(N_{iter}(N_{cg}M_t^2+K^2M_t^2)\right)$	5.68E8	S_k: Size of convolutional kernel
General Framework	$O\left(NM_tKS_kN_k+(N_f+K)N_h+N_{cg}(KM_t^2+K^2)\right)$	8.46E7	N_k: Number of convolutional kernel
Low-complexity	$O\left(N_{cg}K^2+K^2M+N_{cg}KM_t^2\right)$	1.34E7	N_f: Input size of fully-connected
Robust SLNR	$O\left(N_{cg}KM_t^2\right)$	1.31E7	N_h: Number of hidden layers neurons
Robust RZF	$O\left(M_t^3+KM_t^2\right)$	2.75E6	N_{cg}: Iterative number in CG method

i.e., **S2** achieves the same SINRs as **S1**. In addition, obviously **S1** is a flexible solution for **P2** so that the optimal solution **S2** achieve lower or equal objective (total power).

When **S1** is global optimal, obviously **S2** is also optimal for **P1**, as it achieves the same objective as **S1**. This completes the proof.

APPENDIX B
PROOF OF THEOREM 1

Let $\lambda_k^{[n_k]}$ denote the n_k-th largest generalized eigenvalue of matrix pair $(\mathbf{S}_k,\mathbf{N}_k)$, we have

$$\mu_k\mathbf{R}_k\underline{\mathbf{p}}_k^{[n_k]}=\lambda_k^{[n_k]}\Big(\sigma_n^2\mathbf{I}+\sum_{i\neq k}^{K}\mu_i\mathbf{R}_i\Big)\underline{\mathbf{p}}_k^{[n_k]},\forall k. \tag{56}$$

Construct the precoding vector $\mathbf{p}_k^{[n_k]}=\sqrt{\rho_k^{[n_k]}}\underline{\mathbf{p}}_k^{[n_k]}$, where $\rho_k^{[n_k]},\forall k$ satisfies the following equations

$$\begin{aligned}&\sigma_n^2+\sum_{i\neq k}^{K}(\underline{\mathbf{p}}_i^{[n_i]})^H\mathbf{R}_k\underline{\mathbf{p}}_i^{[n_i]}\cdot\rho_i^{[n_i]}\\&\quad-\frac{1}{\lambda_k^{[n_k]}}(\underline{\mathbf{p}}_k^{[n_k]})^H\mathbf{R}_k\underline{\mathbf{p}}_k^{[n_k]}\cdot\rho_k^{[n_k]}=0,\ \ \forall k.\end{aligned} \tag{57}$$

Similar to Lemma 2, $\rho_k^{[n_k]}$ uniquely exists. Let (56) left-multiplied by $\rho_k^{[n_k]}(\underline{\mathbf{p}}_k^{[n_k]})^H/\sigma_n^2$ and let (57) left-multiplied by μ_k/σ_n^2, then sum up these equations of all users, we have

$$\begin{aligned}&\sum_{k=1}^{K}(1+\frac{1}{\lambda_k^{[n_k]}})\frac{\mu_k}{\sigma_n^2}(\mathbf{p}_k^{[n_k]})^H\mathbf{R}_k\mathbf{p}_k^{[n_k]}\\&\quad=\sum_{k=1}^{K}\Big(\rho_k^{[n_k]}+\sum_{i=1}^{K}\frac{\mu_i}{\sigma_n^2}(\mathbf{p}_k^{[n_k]})^H\mathbf{R}_i\mathbf{p}_k^{[n_k]}\Big),\end{aligned} \tag{58}$$

$$\begin{aligned}&\sum_{k=1}^{K}(1+\frac{1}{\lambda_k^{[n_k]}})\frac{\mu_k}{\sigma_n^2}(\mathbf{p}_k^{[n_k]})^H\mathbf{R}_k\mathbf{p}_k^{[n_k]}\\&\quad=\sum_{k=1}^{K}\Big(\mu_k+\sum_{i=1}^{K}\frac{\mu_k}{\sigma_n^2}(\mathbf{p}_i^{[n_i]})^H\mathbf{R}_k\mathbf{p}_i^{[n_i]}\Big).\end{aligned} \tag{59}$$

By combining the results, we have

$$\sum_{k=1}^{K}\mu_k=\sum_{k=1}^{K}\rho_k^{[n_k]}\leq P,\ \ \forall n_k, \tag{60}$$

where the sign '$\leq$' is because that one set of $\{\rho_k^{[n_k]}\}$ is the power of optimal solution. This means for arbitrary n_k, $\mathbf{p}_1^{[n_1]},\ldots,\mathbf{p}_K^{[n_K]}$ can achieve the minimum power although it may not be flexible.

Assume that γ_k is not the maximum generalized eigenvalues, then there always exists another eigenvector of a larger eigenvalue, which simultaneously achieves the minimum total power and higher SINR, while the SINRs of other users remain unchanged because of the power control of (57). Similar to Appendix A, we can reduce the power of this user to achieve lower total power and simultaneously still satisfy the constraints, resulting in the contradiction. Thus, γ_k is the maximum generalized eigenvalue. This completes the proof.

APPENDIX C
PROOF OF LEMMA 2

Denote the matrix $\mathbf{Q}=\mathbf{T}\mathbf{\Lambda}$, where $\mathbf{\Lambda}$ is diagonal and with $[\mathbf{\Lambda}]_{kk}=\rho_k$. According to (31), we have

$$\sum_{j\neq k}^{K}q_{kj}=q_{kk}-1<q_{kk},\ \ k=1,\ldots,K, \tag{61}$$

where $[\mathbf{Q}]_{ki}=q_{ki}$. This means the matrix $\mathbf{Q}$ is strictly diagonally dominant. Thus, we have that $\mathbf{Q}$ is non-singular [59, Theorem 6.1.10 (a)]. As $\mathbf{\Lambda}\succ\mathbf{0}$ is non-singular, the matrix $\mathbf{T}=\mathbf{Q}\mathbf{\Lambda}^{-1}$ is non-singular. This completes the proof.

APPENDIX D
PROOF OF THEOREM 2

As proved in Appendix B, for all $\mu_k,k=1,\ldots,K$ which satisfying $\sum_{k=1}^{K}\mu_k\leq P$, a set of precoding vectors $(\mathbf{p}_1,\ldots,\mathbf{p}_K)$ satisfying $\sum_{k=1}^{K}\mathbf{p}_k^H\mathbf{p}_k\leq P$ can be constructed using the structure in (25a) and (34). The corresponding SINRs satisfy $\mathrm{SINR}_k=\rho\big(\mathbf{N}_k^{-1}\mathbf{S}_k\big),\forall k$; thus, the corresponding upper bounds of ergodic rates satisfy

$$\mathcal{R}_k^{ub}=\log(1+\mathrm{SINR}_k)=\check{\mathcal{R}}_k,\forall k. \tag{62}$$

Similarly, for all $(\mathbf{p}_1,\ldots,\mathbf{p}_K)$ satisfying $\sum_{k=1}^{K}\mathbf{p}_k^H\mathbf{p}_k\leq P$, we can construct the corresponding Lagrange multipliers satisfying $\sum_{k=1}^{K}\mu_k\leq P$ by (44).

In the following, we use the superscript $\star$ and $\diamond$ to denote the optimal solutions (and their derivates) of **P1** and **P4**, respectively. As $(\mu_1^{\diamond},\ldots,\mu_K^{\diamond})$ is optimal for **P4**, we have

$$f(\check{\mathcal{R}}_1^{\diamond},\ldots,\check{\mathcal{R}}_K^{\diamond})\geq f(\check{\mathcal{R}}_1^{\star},\ldots,\check{\mathcal{R}}_K^{\star}). \tag{63}$$

As $(\mathbf{p}_1^{\star},\ldots,\mathbf{p}_K^{\star})$ is optimal for **P1**, we have

$$f(\mathcal{R}_1^{ub\star},\ldots,\mathcal{R}_K^{ub\star})\geq f(\mathcal{R}_1^{ub\diamond},\ldots,\mathcal{R}_K^{ub\diamond}). \tag{64}$$

Combine (62) - (64), we have

$$f(\mathcal{R}_1^{ub\star},\ldots,\mathcal{R}_K^{ub\star}) = f(\mathcal{R}_1^{ub\diamond},\ldots,\mathcal{R}_K^{ub\diamond}), \tag{65}$$

which means the precoding vectors $(\mathbf{p}_1^{\diamond},\ldots,\mathbf{p}_K^{\diamond})$ constructed by $(\mu_1^{\diamond},\ldots,\mu_K^{\diamond})$ achieve the maximum objective of $\mathbf{P1}$. Besides, as proved in Appendix B, we have

$$\sum_{k=1}^{K}(\mathbf{p}_k^{\diamond})^H\mathbf{p}_k^{\diamond} = \sum_{k=1}^{K}\mu_k^{\diamond} \le P, \tag{66}$$

which means $(\mathbf{p}_1^{\diamond},\ldots,\mathbf{p}_K^{\diamond})$ is feasible for $\mathbf{P1}$.

Thus, the precoding vectors constructed by the structure in (25a) and (34) using $\{\mu_k^{\diamond}\}$ is the optimal solution of $\mathbf{P1}$. This completes the proof.

REFERENCES

[1] J. Shi, W. Wang, X. Yi, X. Gao, and G. Y. Li, "Deep learning based robust precoder design for massive MIMO downlink," in *Proc. IEEE Int. Conf. Commun. (ICC)*, Aug. 2021, pp. 1–6.

[2] B. Clerckx, H. Joudeh, C. Hao, M. Dai, and B. Rassouli, "Rate splitting for MIMO wireless networks: a promising phy-layer strategy for LTE evolution," *IEEE Commun. Mag.*, vol. 54, no. 5, pp. 98–105, 2016.

[3] S. Jacobsson, G. Durisi, M. Coldrey, T. Goldstein, and C. Studer, "Quantized precoding for massive MU-MIMO," *IEEE Trans. Commun.*, vol. 65, no. 11, pp. 4670–4684, Nov. 2017.

[4] S. Wagner, R. Couillet, M. Debbah, and D. T. M. Slock, "Large system analysis of linear precoding in correlated MISO broadcast channels under limited feedback," *IEEE Trans. Inf. Theory*, vol. 58, no. 7, pp. 4509–4537, Jul. 2012.

[5] M. Sadek, A. Tarighat, and A. H. Sayed, "Active antenna selection in multiuser MIMO communications," *IEEE Trans. Signal Process.*, vol. 55, no. 4, pp. 1498–1510, Apr. 2007.

[6] S. S. Christensen, R. Agarwal, E. de Carvalho, and J. M. Cioffi, "Weighted sum-rate maximization using weighted MMSE for MIMO-BC beamforming design," *IEEE Trans. Wireless Commun.*, vol. 7, no. 12-1, pp. 4792–4799, Dec. 2008.

[7] G. Caire, N. Jindal, M. Kobayashi, and N. Ravindran, "Multiuser MIMO achievable rates with downlink training and channel state feedback," *IEEE Trans. Inf. Theory*, vol. 56, no. 6, pp. 2845–2866, 2010.

[8] S. Vishwanath, N. Jindal, and A. J. Goldsmith, "Duality, achievable rates, and sum-rate capacity of gaussian MIMO broadcast channels," *IEEE Trans. Inf. Theory*, vol. 49, no. 10, pp. 2658–2668, 2003.

[9] N. Jindal, W. Rhee, S. Vishwanath, S. A. Jafar, and A. J. Goldsmith, "Sum power iterative water-filling for multi-antenna gaussian broadcast channels," *IEEE Trans. Inf. Theory*, vol. 51, no. 4, pp. 1570–1580, 2005.

[10] D. Park, "Sum rate maximisation with transmit antenna selection in massive MIMO broadcast channels," *Electronics Lett.*, vol. 54, no. 21, pp. 1245–1247, 2018.

[11] Q. Li and L. Yang, "Beamforming for cooperative secure transmission in cognitive two-way relay networks," *IEEE Trans. Inf. Forensics Secur.*, vol. 15, pp. 130–143, 2020.

[12] A. Kammoun, A. Müller, E. Björnson, and M. Debbah, "Linear precoding based on polynomial expansion: Large-scale multi-cell MIMO systems," *J. Sel. Topics Signal Process.*, vol. 8, no. 5, pp. 861–875, Oct. 2014.

[13] L. You, X. Gao, X. Xia, N. Ma, and Y. Peng, "Pilot reuse for massive MIMO transmission over spatially correlated rayleigh fading channels," *IEEE Trans. Wireless Commun.*, vol. 14, no. 6, pp. 3352–3366, 2015.

[14] D. Mi, M. Dianati, L. Zhang, S. Muhaidat, and R. Tafazolli, "Massive MIMO performance with imperfect channel reciprocity and channel estimation error," *IEEE Trans. Commun.*, vol. 65, no. 9, pp. 3734–3749, 2017.

[15] A. Lu, X. Gao, W. Zhong, C. Xiao, and X. Meng, "Robust transmission for massive MIMO downlink with imperfect CSI," *IEEE Trans. Commun.*, vol. 67, no. 8, pp. 5362–5376, Aug. 2019.

[16] W. Weichselberger, M. Herdin, H. Ozcelik, and E. Bonek, "A stochastic MIMO channel model with joint correlation of both link ends," *IEEE Trans. Wireless Commun.*, vol. 5, no. 1, pp. 90–100, Jan. 2006.

[17] A.-A. Lu, X. Gao, and C. Xiao, "Robust precoder design for 3D massive MIMO downlink with a posteriori channel model," arXiv:2004.04331 [cs.IT], 2020.

[18] Z. Qin, H. Ye, G. Y. Li, and B. F. Juang, "Deep learning in physical layer communications," *IEEE Wireless Commun.*, vol. 26, no. 2, pp. 93–99, Apr. 2019.

[19] H. He, C. Wen, S. Jin, and G. Y. Li, "Deep learning-based channel estimation for beamspace mmwave massive MIMO systems," *IEEE Wireless Commun. Lett.*, vol. 7, no. 5, pp. 852–855, Oct. 2018.

[20] H. Ye, G. Y. Li, and B. Juang, "Power of deep learning for channel estimation and signal detection in OFDM systems," *IEEE Wireless Commun. Lett.*, vol. 7, no. 1, pp. 114–117, Feb. 2018.

[21] H. He, C. Wen, S. Jin, and G. Y. Li, "Model-driven deep learning for MIMO detection," *IEEE Trans. Signal Process.*, vol. 68, pp. 1702–1715, Mar. 2020.

[22] X. Zhang and M. Vaezi, "Deep learning based precoding for the MIMO gaussian wiretap channel," in *Proc. IEEE Globecom Workshops*, 2019, pp. 1–6.

[23] F. A. Aoudia and J. Hoydis, "Model-free training of end-to-end communication systems," *IEEE J. Sel. Areas Commun.*, vol. 37, no. 11, pp. 2503–2516, Nov. 2019.

[24] H. Ye, L. Liang, G. Y. Li, and B. Juang, "Deep learning-based end-to-end wireless communication systems with conditional GANs as unknown channels," *IEEE Trans. Wireless Commun.*, vol. 19, no. 5, pp. 3133–3143, May. 2020.

[25] H. Ye, G. Y. Li, and B. F. Juang, "Deep reinforcement learning based resource allocation for V2V communications," *IEEE Trans. Veh. Technol.*, vol. 68, no. 4, pp. 3163–3173, Apr. 2019.

[26] L. Liang, H. Ye, G. Yu, and G. Y. Li, "Deep-learning-based wireless resource allocation with application to vehicular networks," *Proc. IEEE*, vol. 108, no. 2, pp. 341–356, Feb. 2020.

[27] X. Zhang and M. Vaezi, "Multi-objective dnn-based precoder for mimo communications," *IEEE Trans. Commun.*, Apr. 2021.

[28] ——, "A DNN-based multi-objective precoding for gaussian MIMO networks," in *IEEE Global Commun. Conf, (GLOBECOM)*, Jan. 2021, pp. 1–6.

[29] X. Li and A. Alkhateeb, "Deep learning for direct hybrid precoding in millimeter wave massive MIMO systems," in *IEEE Asilomar Conf. Signals Systems Comput. (ACSCC)*, M. B. Matthews, Ed., Mar. 2020, pp. 800–805.

[30] H. Huang, Y. Song, J. Yang, G. Gui, and F. Adachi, "Deep-learning-based millimeter-wave massive MIMO for hybrid precoding," *IEEE Trans. Veh. Technol.*, vol. 68, no. 3, pp. 3027–3032, 2019.

[31] W. Xia, G. Zheng, Y. Zhu, J. Zhang, J. Wang, and A. P. Petropulu, "A deep learning framework for optimization of MISO downlink beamforming," *IEEE Trans. Commun.*, 2019.

[32] A. G. Pathapati, N. Chakradhar, P. Havish, S. A. Somayajula, and S. Amuru, "Supervised deep learning for MIMO precoding," in *IEEE 5G World Forum (5GWF)*, Oct. 2020, pp. 418–423.

[33] C. Zhang, P. Patras, and H. Haddadi, "Deep learning in mobile and wireless networking: A survey," *IEEE Commun. Surveys Tuts.*, vol. 21, no. 3, pp. 2224–2287, thirdquarter 2019.

[34] W. Yu, "Sum-capacity computation for the gaussian vector broadcast channel via dual decomposition," *IEEE Trans. Inf. Theory*, vol. 52, no. 2, pp. 754–759, 2006.

[35] Y. Huang and D. P. Palomar, "Rank-constrained separable semidefinite programming with applications to optimal beamforming," *IEEE Trans. Signal Process.*, vol. 58, no. 2, pp. 664–678, 2010.

[36] E. Björnson, M. Bengtsson, and B. E. Ottersten, "Optimal multiuser transmit beamforming: A difficult problem with a simple solution structure [lecture notes]," *IEEE Signal Process. Mag.*, vol. 31, no. 4, pp. 142–148, Jul. 2014.

[37] J. Song, J. Choi, T. Kim, and D. J. Love, "Advanced quantizer designs for FDD-based FD-MIMO systems using uniform planar arrays," *IEEE Trans. on Signal Process.*, vol. 66, no. 14, pp. 3891–3905, 2018.

[38] A.-A. Lu, X. Gao, X. Meng, and X.-G. Xia, "Omnidirectional precoding for 3D massive MIMO with uniform planar arrays," *IEEE Trans. Wireless Commun.*, vol. 19, no. 4, pp. 2628–2642, 2020.

[39] 3GPP TS 38.211 V15.8.0, "NR; physical channels and modulation," Dec. 2019.

[40] D. Ying, F. W. Vook, T. A. Thomas, D. J. Love, and A. Ghosh, "Kronecker product correlation model and limited feedback codebook design in a 3D channel model," in *Proc. IEEE Int. Conf. Commun. (ICC)*, Jun. 2014, pp. 5865–5870.

[41] X. Gao, B. Jiang, X. Li, A. B. Gershman, and M. R. McKay, "Statistical eigenmode transmission over jointly correlated mimo channels," *IEEE Trans. Inf. Theory*, vol. 55, no. 8, pp. 3735–3750, 2009.

[42] M. Series, "Guidelines for evaluation of radio interface technologies for IMT-2020," 2017.

[43] C. Sun, X.-Q. Gao, and Z. Ding, "BDMA in multicell massive MIMO communications: Power allocation algorithms," *IEEE Trans. Signal Process.*, vol. 65, no. 11, pp. 2962–2974, Jun. 2017.

[44] A. Goldsmith, S. A. Jafar, N. Jindal, and S. Vishwanath, "Capacity limits of MIMO channels," *IEEE J. Sel. Areas Commun.*, vol. 21, no. 5, pp. 684–702, 2003.

[45] S. Boyd and L. Vandenberghe, *Convex Optimization*. New York, NY, USA: Cambridge University Press, 2004.

[46] F. Shu, J. Tong, X. You, C. Gu, and J. Wu, "Adaptive robust Max-SLNR precoder for MU-MIMO-OFDM systems with imperfect CSI," *Science China Inf. Sciences*, vol. 59, no. 6, pp. 062 302:1–062 302:14, 2016.

[47] M. Sadek, A. Tarighat, and A. H. Sayed, "A leakage-based precoding scheme for downlink multi-user MIMO channels," *IEEE Trans. Wirel. Commun.*, vol. 6, no. 5, pp. 1711–1721, 2007.

[48] H. Shen, W. Xu, A. L. Swindlehurst, and C. Zhao, "Transmitter optimization for per-antenna power constrained multi-antenna downlinks: An SLNR maximization methodology," *IEEE Trans. Signal Process.*, vol. 64, no. 10, pp. 2712–2725, 2016.

[49] C. Sun, X.-Q. Gao, S. Jin, M. Matthaiou, Z. Ding, and C. Xiao, "Beam division multiple access transmission for massive MIMO communications," *IEEE Trans. Commun.*, vol. 63, no. 6, pp. 2170–2184, Jun. 2015.

[50] K.-X. Li, L. You, J. Wang, X. Q. Gao, C. G. Tsinos, S. Chatzinotas, and B. Ottersten, "Downlink transmit design in massive MIMO LEO satellite communications," arXiv:2008.05343 [eess.SP], 2020.

[51] I. J. Goodfellow, Y. Bengio, and A. Courville, *Deep Learning*. MIT Press, 2016.

[52] F. Liang, C. Shen, and F. Wu, "An iterative BP-CNN architecture for channel decoding," *J. Sel. Topics Signal Process.*, vol. 12, no. 1, pp. 144–159, Feb. 2018.

[53] Z. Liu, L. Zhang, and Z. Ding, "Exploiting bi-directional channel reciprocity in deep learning for low rate massive MIMO CSI feedback," *IEEE Wireless Commun. Lett.*, vol. 8, no. 3, pp. 889–892, Jun. 2019.

[54] H. Yang, "Conjugate gradient methods for the rayleigh quotient minimization of generalized eigenvalue problems," *Comput.*, vol. 51, no. 1, pp. 79–94, Mar. 1993.

[55] S. Jaeckel, L. Raschkowski, K. Börner, and L. Thiele, "Quadriga: A 3-D multi-cell channel model with time evolution for enabling virtual field trials," *IEEE Trans. Antennas Propag.*, vol. 62, no. 6, pp. 3242–3256, Jun. 2014.

[56] W. Xia, G. Zheng, K. Wong, and H. Zhu, "Model-driven beamforming neural networks," *IEEE Wireless Commun.*, vol. 27, no. 1, pp. 68–75, 2020.

[57] T. Jiang, H. V. Cheng, and W. Yu, "Learning to reflect and to beamform for intelligent reflecting surface with implicit channel estimation," *IEEE J. Sel. Areas Commun.*, 2021.

[58] Z. Wang and W. Chen, "Regularized zero-forcing for multiantenna broadcast channels with user selection," *IEEE Wireless Commun. Lett.*, vol. 1, no. 2, pp. 129–132, 2012.

[59] C. R. J. Roger A. Horn, *Matrix Analysis*, 2nd ed. Cambridge University Press, 2013.

Junchao Shi (Student Member, IEEE) received the B.E. degree in communication engineering from Xidian University, Xi'an, China, in 2016. He is currently working towards the Ph.D degree in the National Mobile Communications Research Laboratory, Southeast University, Nanjing, China. His research interests are mainly on communications, signal processing, and information theory, machine learning with emphasis on massive MIMO communications.

Wenjin Wang (Member, IEEE) received the Ph.D. degree in communication and information systems from Southeast University, Nanjing, China, in 2011. From 2010 to 2014, he was with the School of System Engineering, University of Reading, Reading, U.K. He is currently an Associate Professor with the National Mobile Communications Research Laboratory, Southeast University. His research interests include advanced signal processing for future wireless communications and satellite communications. He was awarded a Best Paper Award at IEEE WCSP'09. He was also awarded the first grade Technological Invention Award of the State Education Ministry of China in 2009.

Xinping Yi (Member, IEEE) received the Ph.D. degree in electronics and communications from Télécom ParisTech, Paris, France, in 2015. He is currently a Lecturer (Assistant Professor) with the Department of Electrical Engineering and Electronics, University of Liverpool, U.K. Prior to Liverpool, he was a Research Associate with Technische Universität Berlin, Berlin, Germany, from 2014 to 2017, a Research Assistant with EURECOM, Sophia Antipolis, France, from 2011 to 2014, and a Research Engineer with Huawei Technologies, Shenzhen, China, from 2009 to 2011. His main research interests include information theory, graph theory, and machine learning, and their applications in wireless communications and artificial intelligence.

Xiqi Gao (Fellow, IEEE) received the Ph.D. degree in electrical engineering from Southeast University, Nanjing, China, in 1997.

He joined the Department of Radio Engineering, Southeast University, in April 1992. Since May 2001, he has been a professor of information systems and communications. From September 1999 to August 2000, he was a visiting scholar at Massachusetts Institute of Technology, Cambridge, and Boston University, Boston, MA. From August 2007 to July 2008, he visited the Darmstadt University of Technology, Darmstadt, Germany, as a Humboldt scholar. His current research interests include broadband multicarrier communications, massive MIMO wireless communications, satellite communications, optical wireless communications, information theory and signal processing for wireless communications. From 2007 to 2012, he served as an Editor for the IEEE Transactions on Wireless Communications. From 2009 to 2013, he served as an Associate Editor for the IEEE Transactions on Signal Processing. From 2015 to 2017, he served as an Editor for the IEEE Transactions on Communications.

Dr. Gao received the Science and Technology Awards of the State Education Ministry of China in 1998, 2006 and 2009, the National Technological Invention Award of China in 2011, the Science and Technology Award of Jiangsu Province of China in 2014, and the 2011 IEEE Communications Society Stephen O. Rice Prize Paper Award in the field of communications theory.

Geoffrey Ye Li (Fellow, IEEE) has been a Chair Professor at Imperial College London, UK, since 2020. Before moving to Imperial, he was a Professor with Georgia Institute of Technology in Georgia, USA, for 20 years and a Principal Technical Staff Member with AT&T Labs - Research in New Jersey, USA, for five years. His general research interests include statistical signal processing and machine learning for wireless communications. In the related areas, he has published over 600 journal and conference papers in addition to over 40 granted patents and several books. His publications have been cited over 48,000 times and he has been recognized as a Highly Cited Researcher, by Thomson Reuters, almost every year.

Dr. Geoffrey Ye Li was awarded IEEE Fellow for his contributions to signal processing for wireless communications in 2005. He won several prestigious awards from IEEE Signal Processing Society (Donald G. Fink Overview Paper Award in 2017), IEEE Vehicular Technology Society (James Evans Avant Garde Award in 2013 and Jack Neubauer Memorial Award in 2014), and IEEE Communications Society (Stephen O. Rice Prize Paper Award in 2013, Award for Advances in Communication in 2017, and Edwin Howard Armstrong Achievement Award in 2019). He also received the 2015 Distinguished ECE Faculty Achievement Award from Georgia Tech.

He has been involved in editorial activities for over 20 technical journals, including the founding Editor-in-Chief of IEEE JSAC Special Series on ML in Communications and Networking. He has organized and chaired many international conferences, including technical program vice-chair of the IEEE ICC'03, general co-chair of the IEEE GlobalSIP'14, the IEEE VTC'19 (Fall), and the IEEE SPAWC'20.